

Overview of Results in the MST Reversed-Field Pinch Experiment

D. J. Den Hartog 1), J-W. Ahn 1), A. F. Almagri 1), J. K. Anderson 1), A. D. Beklemishev 2), A. P. Blair 1), F. Bonomo 3), M. T. Borchardt 1), D. L. Brower 4), D. R. Burke 1), M. Cengher 1), B. E. Chapman 1), S. Choi 1), D. J. Clayton 1), W. A. Cox 1), S. K. Combs 5), D. Craig 1), H. D. Cummings 1), V. I. Davydenko 2), D. R. Demers 6), B. H. Deng 4), W. X. Ding 4), F. Ebrahimi 1), D. A. Ennis 1), G. Fiksel 1), C. Foust 5), C. B. Forest 1), P. Franz 3), L. Frassinetti 3), S. Gangadhara 1), J. A. Goetz 1), R. W. Harvey 1), D. J. Holly 1), B. F. Hudson 1), A. A. Ivanov 2), M. C. Kaufman 1), A. V. Kuritsyn 1), A. A. Lizunov 2), T. W. Lovell 1), R. M. Magee 1), L. Marrelli 3), P. Martin 3), K. J. McCollam 1), M. C. Miller 1), V. V. Mirnov 1), P. D. Nonn 1), R. O'Connell 1), S. P. Oliva 1), P. Piovesan 3), S. C. Prager 1), I. Predebon 3), J. A. Reusch 1), J. S. Sarff 1), V. A. Svidzinski 1), T. D. Tharp 1), M. A. Thomas 1), Yu. A. Tsidulko 2), E. Uchimoto 7), M. D. Wyman 1), T. Yates 4)

- 1) The University of Wisconsin–Madison, Madison, Wisconsin, and the Center for Magnetic Self-Organization in Laboratory and Astrophysical Plasmas
- 2) Budker Institute of Nuclear Physics, Novosibirsk, Russia
- 3) Consorzio RFX, Associazione EURATOM-ENEA sulla Fusione, Padova, Italy
- 4) The University of California at Los Angeles, Los Angeles, California
- 5) The Oak Ridge National Laboratory, Oak Ridge, Tennessee
- 6) Rensselaer Polytechnic Institute, Troy, New York
- 7) The University of Montana, Missoula, Montana

E-mail contact of main author: djdenhar@wisc.edu

Abstract. In the general area of confinement improvement and concept advancement, recent results in the MST reversed-field pinch include 1) improved confinement at 500 kA plasma current, with copious energetic electrons and sustained elevated ion temperature greater than 1 keV; 2) raised density in improved-confinement plasmas from injection of frozen deuterium pellets; 3) sustainment of 10% of the plasma current by oscillating field current drive (ac helicity injection), in agreement with theory for the applied power; 4) wave injection from electron Bernstein wave and lower hybrid wave antennas, satisfying theoretical expectations of plasma loading at power levels of about 100 kW. Substantial progress has been made in understanding the causes and effects of magnetic reconnection in the RFP: 1) discovery that fast ions with large gyro-radii are well-confined in the standard RFP, despite the underlying stochasticity of the magnetic field; 2) determination that ion heating during reconnection events appears to be localized to the reconnection layer; 3) observation that global magnetic self-organization (characterized by sudden changes in magnetic energy, plasma momentum, and ion temperature) occurs only when spontaneous ($m = 1$) and driven ($m = 0$) reconnection are present simultaneously. Diagnostic system development continues, including charge-exchange recombination spectroscopy for fluctuation measurement, multi-point and multi-pulse Thomson scattering, spectral motional Stark effect measurement of low-field $|B|$, and multi-color soft x-ray detector arrays for tomographic measurement of time-resolved electron temperature.

1. Introduction

Recent research on the MST reversed-field pinch (RFP) has advanced the concept by demonstrating good ion energy confinement, high density/high beta operation, and a possible plasma current sustainment technique. The RFP can be broadly defined as “toroidal plasma confinement with a low magnetic field” [1]. The toroidal field of an RFP is typically ~ 10 times smaller than a similar plasma current tokamak; in an RFP $B_\phi \approx B_\theta$ and total $\beta \geq 10\%$. Furthermore, in an RFP the toroidal magnetic field goes to zero and then reverses sign near the edge of the plasma. Self-generated plasma currents that drive magnetic reconnection substantially determine the magnetic field equilibrium.

The Madison Symmetric Torus (MST) is a large RFP with major radius $R = 1.5$ m, minor radius $a = 0.5$ m, and a thick (5 cm) aluminum conducting shell [2]. Typical plasma parameter ranges in MST are toroidal plasma current I_p 0.2–0.6 MA, $|\mathbf{B}| \leq 0.5$ T, electron density n_e $0.5\text{--}3 \times 10^{13}$ cm⁻³, and electron T_e and ion T_i temperatures 0.1–2 keV. A typical plasma discharge is approximately 70 msec in duration, with a 20–30 msec “flat-top” in which the plasma current is nearly constant and the plasma is approximately in equilibrium.

The first main section of this paper describes recent results from MST in the general area of confinement improvement and concept advancement. The second main section describes the progress that has been made in understanding the causes and effects of magnetic reconnection in the RFP. The last section is a brief summary of recent diagnostic advances on MST.

2. Confinement Improvement and Concept Advancement

2.1. Improved Confinement at High Current

Recent high-current improved-confinement plasmas in the MST RFP exhibit sustained electron and ion temperatures greater than 1 keV. Previously only increased T_e has been observed during improved-confinement operation; T_i remained at a few hundred eV [3,4]. These new improved-confinement plasmas are produced by applying inductive edge current drive to 500 kA RFP discharges in MST. This edge current replaces fluctuation-driven current, thus the plasma is more stable [5]. Magnetic fluctuations are reduced, energy confinement increases ten-fold, and magnetic relaxation phenomena are strongly reduced.

At this high plasma current, the increase in ion temperature that occurs during magnetic reconnection events in standard RFP operation is much larger than at lower plasma current, and T_i is sustained at a high level during the improved-confinement period (Fig. 1). Substantial neutron flux from majority D-D ion reactions is recorded for the first time in MST, consistent with elevated ion temperature, perhaps even a fast ion component. Without the improved-confinement period, the ion temperature quickly drops following a reconnection event in a standard RFP plasma. During the improved-confinement period, the hard x-ray flux increases to a peak that is 3 to 4 orders of magnitude larger than previously observed. This is indicative of increased electron confinement and/or heating; according to Fokker-Planck modeling at least 10-20% of electron energy is stored in the fast electrons.

2.2. Raised Density in Improved-Confinement Plasmas

Increasing the electron density during high-current improved-confinement operation appears to shift energy from the fast to the bulk electrons (Fig. 2). Injection of frozen deuterium pellets [6] increases density by over 300% in improved-confinement plasmas, while maintaining magnetic fluctuations at a reduced level (Fig. 3). Total beta (including both electron and ion contributions) for these plasmas is 17%, and is 26% for low plasma current operation. During the improved-confinement period T_i rises, likely a result of increased electron-ion coupling.

2.3. Plasma Current by Oscillating Field Current Drive

A major goal of RFP research is the development of techniques for steady-state sustainment of the plasma current and control of the current profile. Oscillating field current drive

(OFCD) is a proposed method for RFP current sustainment using phased oscillations of the surface poloidal and toroidal loop voltages to drive a net emf at the edge of the plasma [7]. This technique is inherently steady-state since the average of these inductive oscillations is zero. Initial tests of OFCD in MST have demonstrated 10% net addition to the plasma current (Fig.4) with ohmic current drive efficiency of ~ 0.1 A/W [8]. Maximum plasma current drive does not occur at maximum helicity injection, but instead occurs when the oscillating voltages are phased such that the amplitude of the edge $m = 0$ MHD tearing mode magnetic fluctuations is minimized (Fig. 5). At this phase the $m = 0$ mode amplitude is below the ‘‘OFCD off’’ case, the amplitude of the core $m = 1$ tearing mode is near a broad minimum, and the total (steady induction plus OFCD) ohmic (dissipated) power is decreased. Nonlinear 3D MHD simulation indicates that OFCD can sustain the full RFP plasma current [9].

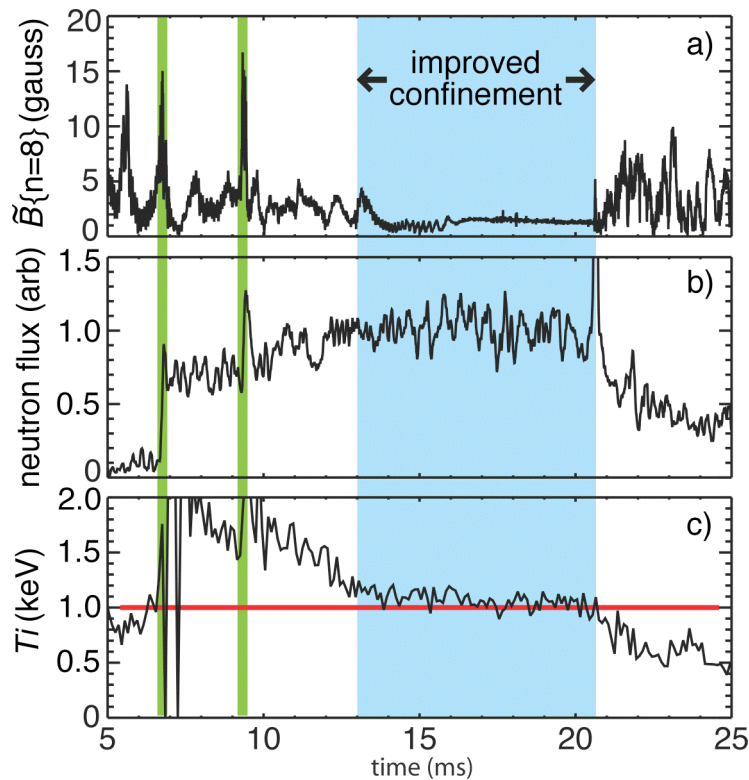


FIG. 1. a) Magnetic fluctuation amplitude, b) D-D neutron emission, and c) C^{+6} impurity ion temperature during an improved confinement plasma. The two vertical shadings at 7 and 9 ms mark reconnection events during which ions are strongly heated.

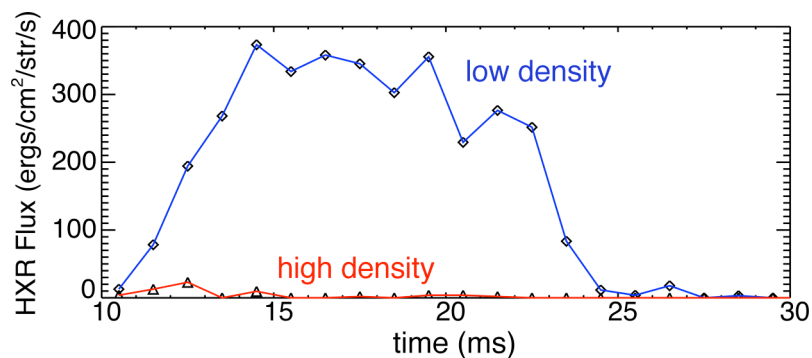


FIG. 2. Hard x-ray (HXR) flux during the improved-confinement period of a low (diamonds) and high (triangles) density plasma. The HXR flux is much lower during the high density case, indicating that the fast electron population is reduced by increased density.

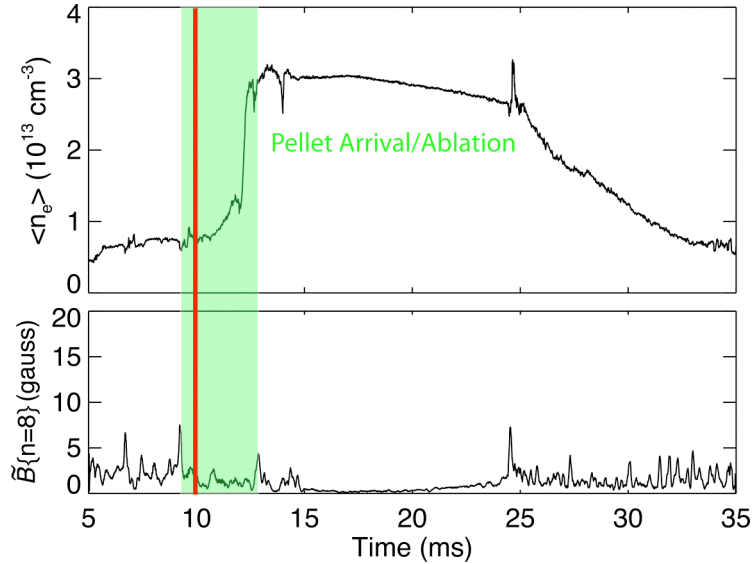


FIG. 3. Injection of a frozen deuterium pellet at the start of an improved-confinement period triples the line-average electron density while magnetic fluctuations are maintained at a reduced level.

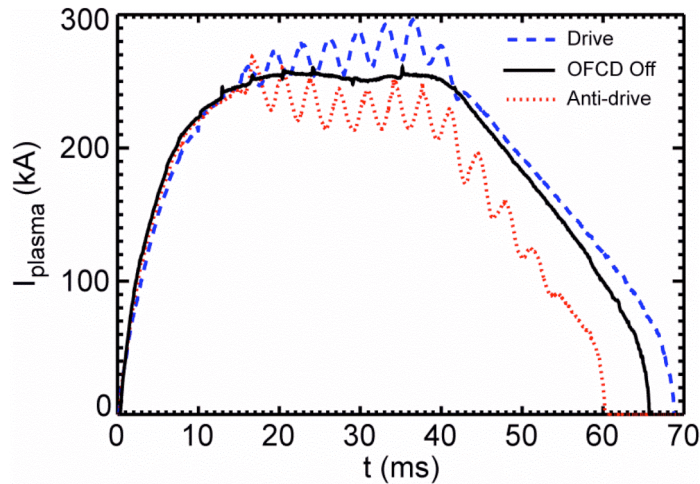


FIG. 4. OFCD adds $\sim 10\%$ to plasma current when phased for current drive, and subtracts an equivalent amount when phased for anti-drive. The added current is limited by the pulse length and the source voltage; both are being increased.

2.4. Electron Bernstein and Lower Hybrid Wave Injection

A possible approach to current-profile control in the RFP is rf current drive. Two rf techniques, lower hybrid (LH) and electron Bernstein wave (EBW), are in the early assessment stage on MST. A working LH antenna is installed on MST, delivering approximately 80 kW at 800 MHz to the plasma [10]. Strong x-ray emission at 20 keV has been seen and may indicate coupling to the plasma; this emission is not expected from direct acceleration by local antenna electric fields [11]. An EBW twin-waveguide antenna has delivered over 100 kW at 3.6 GHz, with a reflection coefficient ~ 0.3 [12]. Coupling efficiency depends sensitively upon several factors, including the edge electron density profile, the polarization (X or O mode), and the phase between the waveguides [13]. Both rf current drive techniques are being extended to the 300 kW level, where measurable changes in hard x-ray emission and other plasma parameters should be observable.

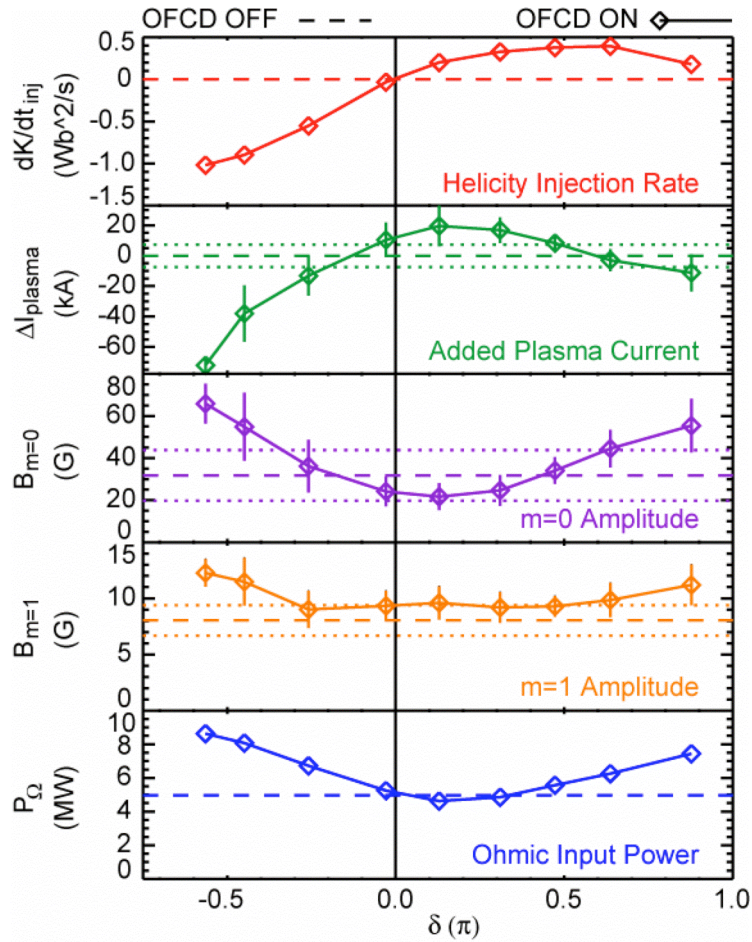


FIG. 5. Maximum plasma current drive occurs when the phase δ between the oscillating voltages is such that the amplitude of the edge $m = 0$ MHD tearing mode magnetic fluctuations is minimized.

3. Magnetic Reconnection in the RFP

Standard RFP plasmas exhibit substantial magnetic reconnection activity driven by multiple tearing modes. The safety factor q is $\ll 1$ on axis and decreases toward the edge, passing through zero and becoming negative; as a result, $m = 1$ tearing modes are resonant on multiple rational surfaces, and form overlapping magnetic islands.

3.1 Fast Ion Confinement

One of the consequences of this fluctuation activity is magnetic stochasticity, yet measured confinement (>20 ms) of injected fast ions is much better than that expected (~ 1 ms) if the ions simply stream along the stochastic field lines [14]. This experimental investigation was carried out with a short-pulse (1.3 ms) of fast (20 keV) D neutrals injected into a D plasma in MST. Fusion D-D neutrons from fast ion/plasma ion collisions were recorded by a scintillator detector. The decay of this neutron signal indicates that the fast ion confinement is >20 ms (Fig. 6); the fast ion slowing down is as expected from classical coulomb collisions with plasma electrons and ions. Full orbit numerical calculation of particle trajectories in the stochastic field of the RFP indicates that these large gyro-orbit ions do not follow the magnetic field lines until they have deposited most of their energy into the plasma; only then are they stochastically transported out of the plasma. This has positive implications for the feasibility of neutral beam injection and alpha-particle confinement.

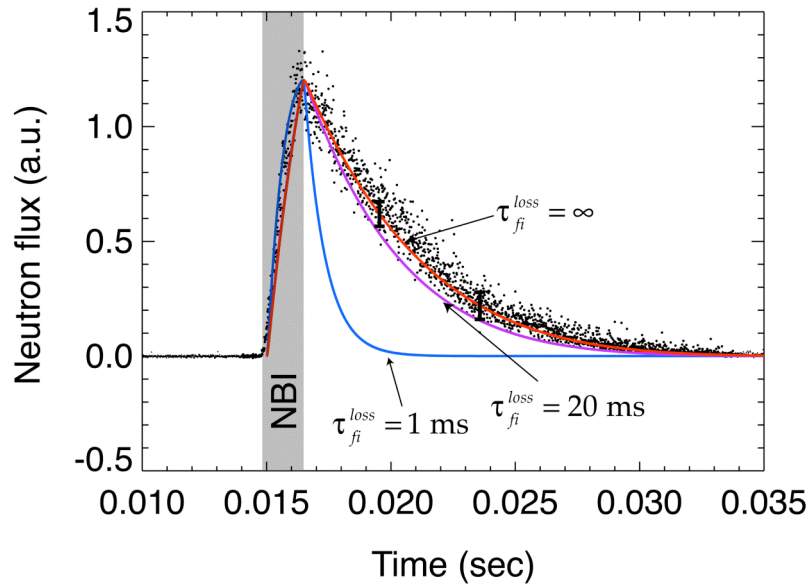


FIG. 6. Comparison of measured neutron signal (dots) and modeling (solid lines). The shaded area represents the neutral beam injection duration. The solid $\tau_{fi}^{loss} = \infty$ line is a result of modeling with classical fast-ion slowing down and perfect ion confinement. The solid $\tau_{fi}^{loss} = 20$ ms and $\tau_{fi}^{loss} = 1$ ms lines show the fits for the corresponding fast-ion confinement times.

3.2 Ion Heating

Another consequence of reconnection activity in the RFP is heating of impurity and majority ions during the bursts of tearing mode fluctuations that occur periodically during a standard RFP discharge. Charge-exchange spectroscopy measurements of the impurity ion temperature profile show that, at moderate plasma current, the ion temperature increases significantly in approximately 100 microseconds [15]. During a global reconnection event in which both core $m = 1$ and edge $m = 0$ tearing modes show a burst of activity, the temperature more than doubles, and the temperature increase is global, occurring throughout the volume of the plasma (Fig. 7). Conversely, during an edge reconnection event involving only the $m = 0$ modes, the temperature increase is smaller and ion heating is limited to the outer half of the plasma (Fig. 8). These results suggest that ion heating is localized near the reconnection layer, and that the large-scale heating observed during a global reconnection event arises from the presence of many reconnection layers distributed throughout the plasma. For both kinds of events, the drop in magnetic energy stored in the plasma is sufficient to account for the increase in ion thermal energy. Rutherford scattering measurements of majority D ion temperature show a smaller increase during a burst, indicating a possible charge and/or mass dependence of the heating mechanism.

3.3 Magnetic Self-Organization

Tearing mode fluctuations also may produce charge transport; this has been measured for the first time in the core of a high-temperature plasma using a high-speed laser-based Faraday rotation diagnostic on MST [16]. Nonlinear coupling between modes enhances the global magnetic self-organization characteristic of the RFP plasma. The self-organization that takes place during these tearing mode bursts occurs only when spontaneous ($m = 1$) and driven ($m = 0$) reconnection is present simultaneously [17].

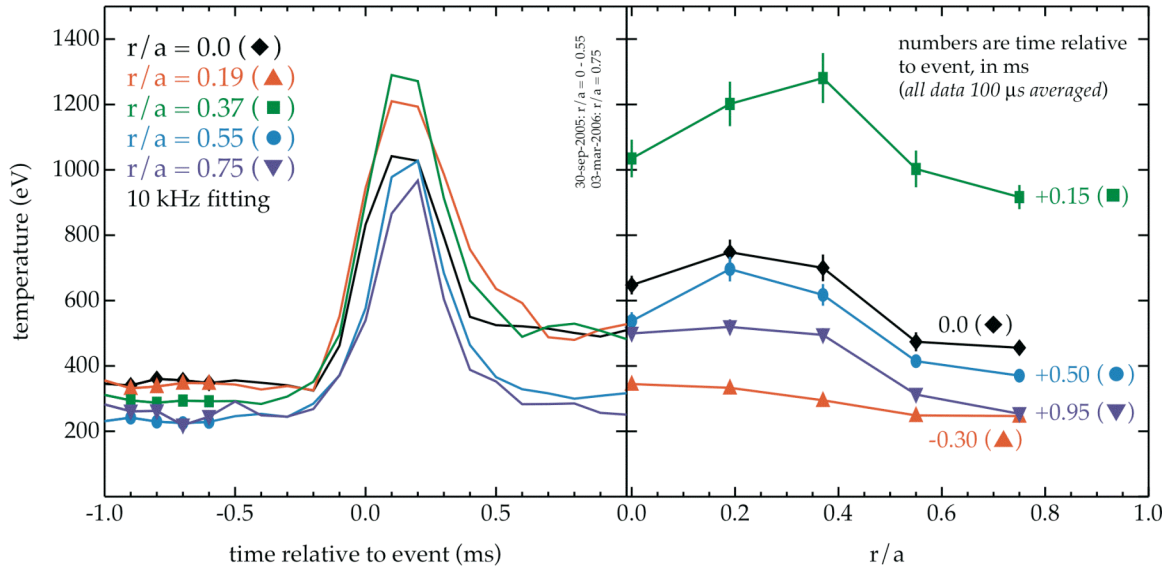


FIG. 7. Left: The impurity (C^{+6}) ion temperature through a global reconnection event. Right: Radial profiles of the impurity ion temperature through a global reconnection event.

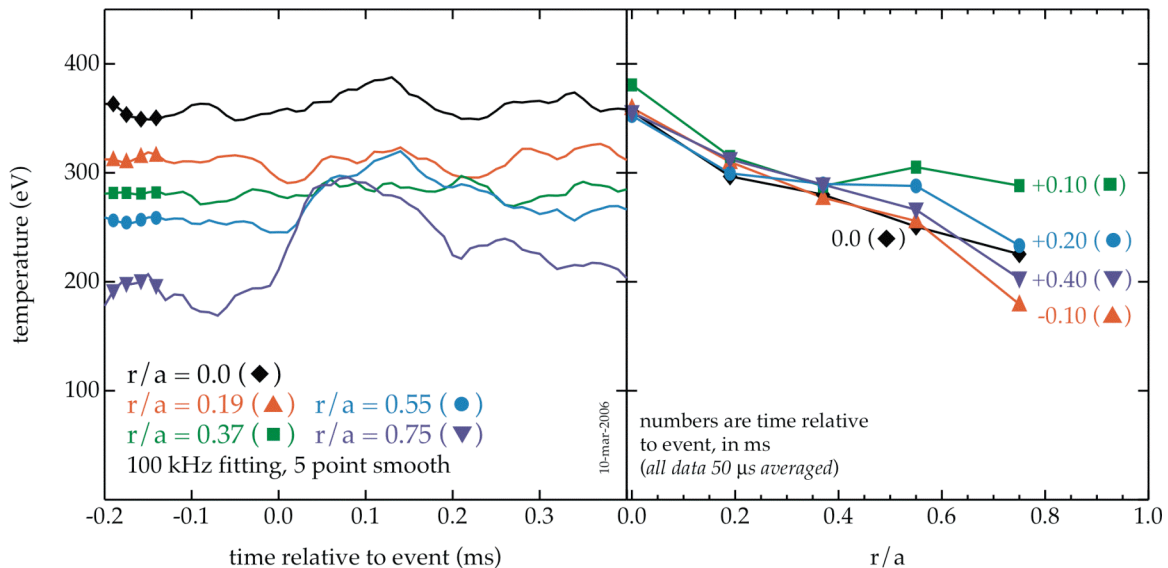


FIG. 8. Left: The impurity (C^{+6}) ion temperature through an edge reconnection event. Right: Radial profiles of the impurity ion temperature through an edge reconnection event.

4. Diagnostic System Development

Diagnostic system development continues, including charge-exchange recombination spectroscopy for fluctuation measurement [18], multi-point and multi-pulse Thomson scattering [19], spectral motional Stark effect measurement of low-field $|\mathbf{B}|$ [20], and multi-color soft x-ray detector arrays for tomographic measurement of time-resolved electron temperature [21].

Acknowledgement

This work is supported by the U. S. Department of Energy and National Science Foundation.

- [1] ORTOLANI, S., and SCHNACK, D.D., *Magnetohydrodynamics of Plasma Relaxation*, World Scientific, Singapore (1993).
- [2] DEXTER, R.N., *et al.*, “The Madison Symmetric Torus,” *Fusion Technol.* **19** (1991) 131.
- [3] CHAPMAN, B.E., *et al.*, “High confinement plasmas in the Madison Symmetric Torus reversed-field pinch,” *Phys. Plasmas* **9** (2002) 2061.
- [4] SARFF, J.S., *et al.*, “Tokamak-like confinement at high beta and low field in the reversed field pinch,” *Plasma Phys. Control. Fusion* **45** (2003) A457; “Tokamak-like confinement at a high beta and low toroidal field in the MST reversed field pinch,” *Nucl. Fusion* **43** (2003) 1684.
- [5] ANDERSON, J.K., *et al.*, “Dynamo-free plasma in the reversed-field pinch: Advances in understanding the reversed-field pinch improved confinement mode,” *Phys. Plasmas* **12** (2005) 056118.
- [6] COMBS, S.K., *et al.*, “New ORNL pellet injection system and installation/initial operations on MST,” *Fusion Sci. Technol.* **44**, (2003) 513.
- [7] M. K. BEVIR, M.K., GIMBLETT, C.G., and MILLER, G., “Quasi-steady-state toroidal discharges,” *Phys. Fluids* **28** (1985) 1826.
- [8] MCCOLLAM, K.J., *et al.*, “Oscillating-Field Current-Drive Experiments in a Reversed Field Pinch,” *Phys. Rev. Lett.* **96** (2006) 035003.
- [9] EBRAHIMI, F., *et al.*, “The three-dimensional magnetohydrodynamics of ac helicity injection in the reversed field pinch,” *Phys. Plasmas* **10** (2003) 999.
- [10] GOETZ, J.A., *et al.*, “Lower hybrid antenna design for MST,” *AIP Conference Proceedings* **787** (2005) 323.
- [11] KAUFMAN, M.C., *et al.*, “Lower hybrid experiments on MST,” *AIP Conference Proceedings* **787** (2005) 319.
- [12] ANDERSON, J.K., *et al.*, “EBW experiments in the Madison Symmetric Torus,” *AIP Conference Proceedings* **787** (2005) 341.
- [13] CENGHER, M., *et al.*, “Coupling to the electron Bernstein wave using a phased array of waveguides in MST reversed field pinch,” *Nucl. Fusion* **46** (2006) 521.
- [14] FIKSEL, G., *et al.*, “Observation of Weak Impact of a Stochastic Magnetic Field on Fast-Ion Confinement,” *Phys. Rev. Lett.* **95** (2005) 125001.
- [15] GANGADHARA, S., *et al.*, “Spatially resolved measurements of ion heating during impulsive reconnection in the Madison Symmetric Torus,” in preparation.
- [16] DING, W.X., *et al.*, “Measurement of the Hall Dynamo Effect during Magnetic Reconnection in a High-Temperature Plasma,” *Phys. Rev. Lett.* **93** (2004) 045002.
- [17] CHOI, S., *et al.*, “Cause of sudden magnetic reconnection in a laboratory plasma,” *Phys. Rev. Lett.* **96** (2006) 145004.
- [18] GANGADHARA, S., *et al.*, “Modeling Fast Charge Exchange Recombination Spectroscopy (CHERS) measurements from the Madison Symmetric Torus (MST),” *Rev. Sci. Instrum.* **77** (2006), in press.
- [19] O’CONNELL, R., *et al.*, “Temporally and spatially resolved electron temperature measurements on the MST reversed-field pinch,” 16th Topical Conference on High-Temperature Plasma Diagnostics (Williamsburg, 2006).
- [20] DEN HARTOG, D.J., *et al.*, “Advances in neutral-beam-based diagnostics on the Madison Symmetric Torus reversed-field pinch (invited),” *Rev. Sci. Instrum.* **77** (2006), in press.
- [21] FRANZ, P., *et al.*, “2-D time resolved measurements of the electron temperature in MST,” *Rev. Sci. Instrum.* **77** (2006), in press.